computation

MDPI

Article

Modeling the Dynamic Effects of Human Mobility and Airborne Particulate Matter on the Spread of COVID-19

Klot Patanarapeelert [1,*], Rossanan Chandumrong [2] and Nichaphat Patanarapeelert [2]

[1] Department of Mathematics, Faculty of Science, Silpakorn Universtiy, Nakhon Pathom 73000, Thailand
[2] Department of Mathematics, Faculty of Applied Science, King Mongkut's University of Technology North Bangkok, Bangkok 10800, Thailand; rose.03346@gmail.com (R.C.); nichaphat.p@sci.kmutnb.ac.th (N.P.)
* Correspondence: klotpat@gmail.com

Abstract: Identifying the relationship between human mobility, air pollution, and communicable disease poses a challenge for impact evaluation and public health planning. Specifically, Coronavirus disease 2019 (COVID-19) and air pollution from fine particulates (PM2.5), by which human mobility is mediated in a public health emergency. To describe the interplay between human mobility and PM2.5 during the spread of COVID-19, we proposed a nonlinear model of the time-dependent transmission rate as a function of these factors. A compartmental epidemic model, together with daily confirmed case data in Bangkok, Thailand during 2020–2021, was used to estimate the intrinsic parameters that can determine the impact on the transmission dynamic of the two earlier outbreaks. The results suggested a positive association between mobility and transmission, but this was strongly dependent on the context and the temporal characteristics of the data. For the ascending phase of an epidemic, the estimated coefficient of mobility variable in the second wave was greater than in the first wave, but the value of the mobility component in the transmission rate was smaller. Due to the influence of the baseline value and PM2.5, the estimated basic reproduction number of the second wave was higher than that of the first wave, even though mobility had a greater influence. For the descending phase, the value of the mobility component in the second wave was greater, due to the negative value of the estimated mobility coefficient. Despite this scaling effect, the results suggest a negative association between PM2.5 and the transmission rates. Although this conclusion agrees with some previous studies, the true effect of PM2.5 remains inconclusive and requires further investigation.

Keywords: COVID-19 pandemic; PM2.5; human mobility; epidemic model

Citation: Patanarapeelert, K.; Chandumrong, R.; Patanarapeelert, N. Modeling the Dynamic Effects of Human Mobility and Airborne Particulate Matter on the Spread of COVID-19. *Computation* **2023**, *11*, 211. https://doi.org/10.3390/computation11110211

Academic Editors: Jacques Demongeot and Kayode Oshinubi

Received: 25 September 2023
Revised: 24 October 2023
Accepted: 27 October 2023
Published: 30 October 2023

1. Introduction

The COVID-19 pandemic, human mobility, and air pollution are mutually interacting issues that require good strategies and adequate preventive measures to mitigate their devastating power amid environmental crises [1]. Although the exact relationship between air pollution and COVID-19 infections is inconclusive, it is evident that exposure to particulate matter (PM), especially with a diameter of 2.5 (PM2.5) may induce accelerated transmission dynamics [2–6]. It is thought that PM2.5 could act as a carrier for droplet nuclei that facilitate the infectiousness of the SARS-CoV-2 in aerosols for hours and on surfaces for days [1]. This results in a high probability of prolonging the virus in the atmosphere [7]. Nevertheless, some studies have reported no significant or a negative association between PM2.5 and COVID-19 case counts [8,9]. It is noted that further evidence is needed, focusing on the long-term effects of integrated meteorological variables, lockdown measures, and population mobility.

Not only are they health-threatening, COVID-19 and air pollution also cause significant changes in lifestyle. Travel restrictions, social distancing, face masks, and limiting public meetings during the pandemic could have had an impact on the spread. In particular, limiting human mobility may also partially affect air pollution [5,10,11]. For example,

the lockdown measures may have caused significant decreases in the concentrations of PM2.5 globally in the range of 2.9–76.5% [12]. Thus, the interaction between human mobility and air pollution should not be neglected, in order to understand the response of transmission dynamics.

Several sources of mobility data developed in recent years contain rich, multi-faceted spatiotemporal information on human mobility patterns. With the rapid growth of telecommunication devices, global positioning systems (GPS) enable the collection of individual mobility data through the GPS position of each mobile phone user. These data have been regularly updated and released to the public for the purpose of supporting public health authorities and the research community in response to COVID-19 [13]. The most commonly used mobility dataset platforms are Google Mobility Reports and Apple Mobility Trends Report. These data have been widely used for the different aims of studies, such as the evaluation of control measures, how people's mobility patterns change when there are restrictions in place, how air pollution changes during lockdowns, etc. [14].

As the characteristics of the epidemic, social behavior, and response policy were diverse across regions and time periods, several models of human mobility have been individually designed and developed to quantify the impact of public health measures [15–18]. A common finding confirms the positive correlation between human mobility and the infection of COVID-19. A ten percentage point reduction in mobility may be associated with a 0.04–0.07 reduction in the value of the effective reproduction number [19]. However, there are a few models that have combined the effect of pollution [5]. Most modeling processes usually apply statistical methods, including advanced regression models [17,20]. However, the result may potentially be misleading if the underlying relationship between the variables is nonlinear [21]. It is also difficult to identify the underlying mechanism as the complexity increases.

In this study, a mixture between data-based and epidemic-compartmental-based modeling was implemented to quantify the effects of human mobility and PM2.5 during the emergence and recurrence of SARS-CoV-2. The susceptible–exposed–infectious–recover model with time-dependent transmission rate was developed. We propose a novel model of time-dependent transmission that depends on the product of a function of human mobility and a nonlinear function of PM2.5 concentration. These two variables are treated as external forces in the model. We aimed to describe the influence of mobility and PM2.5 using estimated intrinsic parameters given a time series of percentage change in mobility, average PM2.5 concentration, and daily confirmed case data. We extracted a dataset of two early outbreaks in Bangkok, Thailand during 2020–2021. Bangkok is the place where the first confirmed case outside China was detected. A review of the early pandemic and an assessment of the intervention in Thailand can be found in the literature [22–26].

2. Materials and Methods

2.1. Data

This study focuses on two early outbreaks in Bangkok, the capital and the most populous city of Thailand. The population size of Bangkok metropolis was about 5.58 and 5.52 million people in 2020 and 2021, respectively, which was about 8.4 percent of the country's population. Bangkok is the place where the first case in the country was detected. Daily confirmed cases were collected from COVID-19 situation reports by the Emergency Operation Center, Department of Disease Control of Thailand. According to the shape of the epidemic curve (see Figure 1a), it is clear that the range of the first outbreak can be determined from 13 January 2020 to 19 May 2020. Unlike the second outbreak, the designation of this early phase is easier than the descending phase. Since the origin of the second nationwide pandemic was in Samut Sakhon province, an area adjacent to Bangkok, the starting point of the epidemic in Bangkok was similar. According to the data, a temporal period with a decline in daily confirmed cases can be observed. Beyond this phase, the number of cases continually increased through the onset of the third outbreak event, and meanwhile, a vaccination campaign was launched. Since we aimed to model

and compare the effect of mobility and PM2.5 on the first wave, as the first step, we defined the period of the second outbreak in Bangkok as from 20 November 2020 to 7 March 2021.

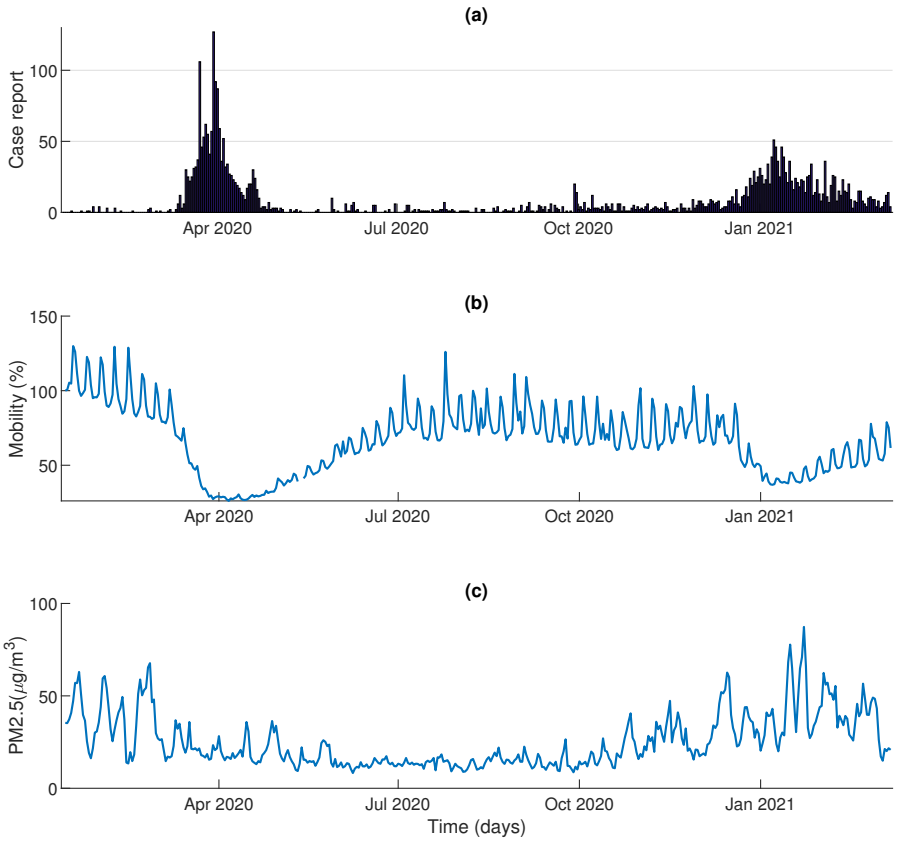

Figure 1. Data presentations in Bangkok for (**a**) the number of daily reported cases, (**b**) the percentage of mobility changes, and (**c**) the daily average PM2.5 density.

The mobility trend reports provided by Apple were used as the estimated change in the volume of people driving, walking, and taking public transit during the pandemic. The measure used was the relative volume of requests for directions in Apple Maps relative to the number of requests occurring on 13 January 2020 [15]. In Figure 1b, we calculated the average of two routes per day to capture the overall percentage change. The weekly cyclic pattern reflects the relatively higher movement volume during the weekend. This trend shows two significant decreases during the two epidemic events, i.e., the first wave lockdown measures in April, and the period between the end of 2020 and January 2021 of the second outbreak. It is noted that, after mobility had reached its relative minimum, the change in volume returned to the average normal level, which was lower than the reference level, i.e., 100% or prior to the pandemic.We can also observe that there were both decreasing and increasing trends in mobility in the descending period in the case report for the the second wave.

The evidence shows that there was an association between the particulate matter and increased incidence and mortality of COVID-19 in various regions [3]. The density data for PM2.5 in the Bangkok metropolis were collected from fourteen distributed ambient air quality monitoring stations of the Thai Pollution Control Department. The 24 h average was calculated per station and the 14-station average was computed, as shown in Figure 1c. The overall fluctuating pattern shows the relatively high pollution during the winter season. Coincidentally, the periods of high pollution coincided with the time of the outbreaks. The average density of PM2.5 in Bangkok showed a bi-week oscillation. The long-term data from 2006 to 2016 reveals that the PM2.5 during the dry season (about October–April) was

higher than in the wet season (about May–September) [27]. This characteristic was also observed during the pandemic event in 2020–2021.

2.2. Time Breaking and Correlation Test

For each outbreak, we aimed to measure the effects of mobility and PM2.5 during two events: i.e., the ascending phase (phase I), when the outbreak commenced until reaching the peak, and the descending phase (phase II) correlated with the decline in the number of cases through to the ceasing or a relatively small number of cases. As the data size matters, this simple partition of time may be suitable for the presented estimation procedure. According to the daily cases report, the separation points were 29 March 2020 for the first wave and 7 January 2021 for the second wave. These separation points were chosen using the local maximum number of daily confirmed cases.

Prior to modeling the relationship between the transmission of COVID-19 and the two variables, i.e., human mobility and PM2.5, we examined whether the number of daily confirmed cases were related to the variables that were thought to affect it. Spearman rank correlation was used to test the correlation, since this is non-parametric and appropriate for ordinal data [28]. The two-way hypothesis test used was as follows: $H_0 : \rho_S = 0$ and $H_A : \rho_S \neq 0$, where ρ_S stands for the Pearson correlation coefficient. The formula for calculating the sampled Spearman correlation coefficient is given by

$$r_S = 1 - \frac{6\sum_i^n d_i^2}{n(n^2-1)},$$

where d_i is the difference in paired orders, and n is the sample size. To this end, the dataset was separately tested according to the aforementioned setting, with a 95% confidence level. The results are given in Table 1.

Table 1. Spearman correlation between the daily reported cases and the input variables.

Phase	Input Variable	r_S	p-Value	Null Hypothesis
		Wave 1		
I	Mobility	−0.6234	1.4030×10^{-9}	Rejected
	PM2.5	−0.3971	3.4870×10^{-4}	Rejected
II	Mobility	−0.8546	1.4930×10^{-15}	Rejected
	PM2.5	0.2496	7.7360×10^{-2}	Rejected
		Wave 2		
I	Mobility	−0.7633	1.8150×10^{-10}	Rejected
	PM2.5	0.1839	2.0590×10^{-1}	Rejected
II	Mobility	−0.4973	6.1470×10^{-5}	Rejected
	PM2.5	0.1290	3.3030×10^{-1}	Rejected

The results indicate that the number of new cases in Bangkok and the population mobility moved in opposite directions, while the number of new cases and PM2.5 had a positive relationship, except for during the first phase of the first wave. Overall, the relationship between the number of cases and mobility was stronger than with PM2.5. It can be seen that, for both variables, there was some degree of association with the number of confirmed cases, as the null hypothesis was rejected. Nevertheless, this was far from justifying the exact relationship, since we ignored the effects of other variables in estimating the correlation coefficient, especially, the cooperative effect of mobility and PM2.5, and the time delay caused by the incubation. Thus, a suitable epidemiological model with a modified time-dependent transmission rate could be proposed [29].

2.3. Mathematical Model

To establish the relationship between the incidence, mobility, and PM2.5, we first developed an epidemiological model by assuming that the transmission rate depended on mobility and PM2.5 (see Figure 2). These two factors were viewed as inputs to the model. A simple epidemiological model was developed of the SEIR type, since an incubation period is usually taken into account [30]. Since we are dealing with a temporal dynamic, i.e., each outbreak was isolated, and the fraction of infected people was small, incorporating the effect of reinfection might be redundant for our purpose. Let $S(t)$ and $E(t)$ be the number of susceptible and exposed population at time t. The recovered group denoted by $R(t)$ can be thought of as the immunized or deceased, and this dynamic can be ignored due to the assumption of a constant population, given by N. Since asymptomatic infection is important, we differentiated the asymptomatic population denoted by I_a from the symptomatic population denoted by I_s. The corresponding transmissibility and recovery rates were also differentiated, whose labels are indicated by subscripts. The dynamical equations of the transmission of COVID-19 can be expressed as

$$\begin{aligned} \frac{dS(t)}{dt} &= -\frac{\beta(t)}{N} S(t)(cI_a(t) + I_s(t)), \\ \frac{dE(t)}{dt} &= \frac{\beta(t)}{N} S(t)(cI_a(t) + I_s(t)) - \sigma E(t), \\ \frac{dI_a(t)}{dt} &= \sigma\alpha E(t) - \gamma_a I_a(t), \\ \frac{dI_s(t)}{dt} &= (1-\alpha)\sigma E(t) - \gamma_s I_s(t), \end{aligned} \tag{1}$$

where c denotes the scaled factor of transmissibility, α denotes the asymptomatic ratio, σ denotes the transfer rate from the exposed class to the infectious class, and γ_i, $i = a, s$ denotes the recovery rate. A summary of the variables and parameters is given in Appendix A.

Figure 2. Modeling the incidence of COVID-19 driven by mobility and PM2.5.

Let $M(t)$ be the percentage change in human mobility at time t, while $P(t)$ is the average density of PM2.5 at time t. We assumed that the transmission rate was a linear function of mobility, but nonlinear (power law) for PM2.5. The effect on the transmission rate was assumed to be the product of these two functions. Thus, the time-dependent transmission rate can be expressed as

$$\beta(t) = \beta_0 \left(1 - b\left[1 - \frac{M(t)}{100}\right]\right) \left(\frac{P(t)}{\max_{t\in[t_0,t_f]} P(t)}\right)^d, \tag{2}$$

where β_0, b, and d are the parameters to be estimated. The baseline parameter, β_0 describes the transmission rate subject to the mobility pattern prior to the emergence of COVID-19. Besides the effect of mobility, the estimated value of β_0 also reflects the contact rate subject to non-pharmaceutical intervention during the epidemic event. The exponent parameter d indicates the contribution of PM2.5 to the transmission. As the effect of mobility is fixed,

the transmission rate is scaled down by the density of PM2.5 if $d > 0$, but it is scaled up if $d < 0$. However, the association of the two effects should be accounted for. To keep the transmission rate nonnegative for this model, we use the constraint

$$b \leq \left(1 - \frac{M(t)}{100}\right)^{-1}, \tag{3}$$

for all t in a time interval of interest.

2.4. Parameter Estimation

To estimate the transmission rate over a time interval, we assumed that the disease occurred independently in different people, and a new case occurring in a short period was proportional to the number of people. This assumption allowed us to use the Poisson distribution for the number of daily reported cases with the mean

$$m(t) = \theta(1 - \alpha)\sigma E(t), \tag{4}$$

where $0 < \theta < 1$ is the fraction of cases reported over the total cases, and the term $1 - \alpha$ indicates the symptomatic infections, which were mostly reported [31]. The term $E(t)$ can be numerically calculated from the model (1), for which the values of the relevant parameters were extracted from previous studies [32–34] (see Appendix A). The reason for choosing a Poisson distribution was that its simple form–a single parameter–greatly simplifies the log-likelihood function, which avoids over-fitting when the number of available data points is small [35].

Let x_i be the number of new cases reported at time t_i, $i = 0, 1, \ldots, n-1$. The log-likelihood function for the Poisson distribution is given by

$$\mathcal{L}(\beta_0, b, d) = \sum_{i=0}^{n-1} -m(t_i) + x_i \ln m(t_i).$$

Thus,

$$(\widehat{\beta_0}, \widehat{b}, \widehat{d}) = \arg \max_{(\beta_0, b, d)} \mathcal{L},$$

gives a solution to the maximum likelihood estimation problem. A flowchart of the parameter estimation algorithm is shown in Appendix A. Analysis of the correlation between the transmission rate and the mobility over multiple lags indicated that high correlations were found with 1-week and 2-week lags [16,19]. We note that the lag effect was ignored in the present model, due to the assumption that the change in the number of contacts should be instantaneous as the mobility changes.

Once the transmission rate is estimated, the time-dependent reproduction number can be computed as

$$R_t = \beta(t)\left(\frac{\alpha c}{\gamma_a} + \frac{(1 - \alpha)}{\gamma_s}\right), \tag{5}$$

where R_0 accounts for the basic reproduction number.

3. Results

Table 2 gives the estimated values and estimation performance for each time interval. In the first period of the epidemic, the estimated baseline transmission of the second wave was higher than that of the first wave, even though the highest daily cases were fewer. Since this parameter mainly relates to the contact rate, two possible explanations link the adaptation of people to the new episode. In other words, the fear lessened, and the public health response was delayed, due to the origin of the outbreak not being in Bangkok. Since the estimated value of the exponent d was negative, the presence of PM2.5 overall magnified the infection and adjusted the baseline transmission rate, where the degree in

the second wave was slightly higher than in the first wave. As seen in the input data, the level of PM2.5 concentration and the scaling effect in the ascending phases of both waves were coherent.

Table 2. Estimation results.

Phase	Parameter	Estimated Value	95%CI	Standard Error	AIC
Wave 1					
I	β_0	0.1032	(0.0705, 0.1512)	0.1948	681.8815
	b	0.9409	(0.8212, 1.0605)	0.0610	
	d	−1.7720	(−2.1868, −1.3573)	0.2116	
II	β_0	0.0742	(0.0338, 0.1626)	0.4005	713.8336
	b	1.2435	(1.1869, 1.300)	0.0289	
	d	−2.1793	(−2.9594, −1.3992)	0.3980	
Wave 2					
I	β_0	0.1673	(0.1069, 0.2618)	0.2284	585.8771
	b	1.3526	(1.2390, 1.4662)	0.0580	
	d	−2.2687	(−2.7176, −1.8198)	0.2290	
II	β_0	0.0091	(0.0051, 0.0162)	0.2940	464.5327
	b	−7.0783	(−10.6588, −3.4978)	1.8268	
	d	−1.2223	(−1.5683, −0.8764)	0.1765	

Although the positive correlation between the time-dependent transmission rate and the mobility, $M(t)$, can be inferred from the results, there was a prominent distinction in terms of scaled factor between the two waves. Since the estimated value of b in the ascending phase of the second wave was greater, the change in the mobility component of the transmission rate in the second wave was faster, namely the linear mobility function was steeper. However, it seemed that the mobility component in the first wave had a greater value for most values of $M(t)$. To verify this, we substituted the estimated values of b into the mobility component and compared between the two waves. It is easy to see that this was true for $26.06\% < M(t) < 100\%$. By inspecting the mobility data, all percent changes in mobility in the second wave satisfied such a range. There were a few days in January 2020 when the percent change in mobility was greater than 100%.

For the descending phase, the estimated baseline transmission in the second wave was lower than in the first wave, showing that the contact rate was relatively low after the new year period. The effect of PM2.5 was, however, opposite to the ascending phase; that is, the degree of the first wave was higher than that of the second wave. This effect may have been caused by the optimization process, which attempted to adjust the baseline value. Interestingly, the estimated value of parameter b was negative in the second wave, which was the best model according to AIC. Although this seems to be contradictory, we argue that during the descending phase of cases being reported, the mobility instead showed an increasing trend. As we pointed out, the descending phase was indeed very temporal and increased to the next level as time passed.We also found that the mobility component in the second wave had a greater value for all $M(t)$ than in the first wave. Theoretically, the probable interval was $19.58\% < M(t) < 100\%$

Figures 3 and 4 show the model predictions and the predicted time-dependent transmission rates (blue lines), respectively. To determine the pure effect of PM2.5, we plotted $\beta(t)$, for which the mobility change was fixed at 100% (green line). In Figure 4a, the couple lines are approximately close to each other, until in the vicinity of the epidemic peak, and the difference was clearer subsequently. This distinction indicates the effect of the mobility component. Prior to the peak, the fluctuation of $\beta(t)$ largely followed the PM2.5 pattern, even though the mobility continually decreased. We observed that the mobility component was prominently effective from the middle of March 2020, when the percentage changes initially dropped below 50%.

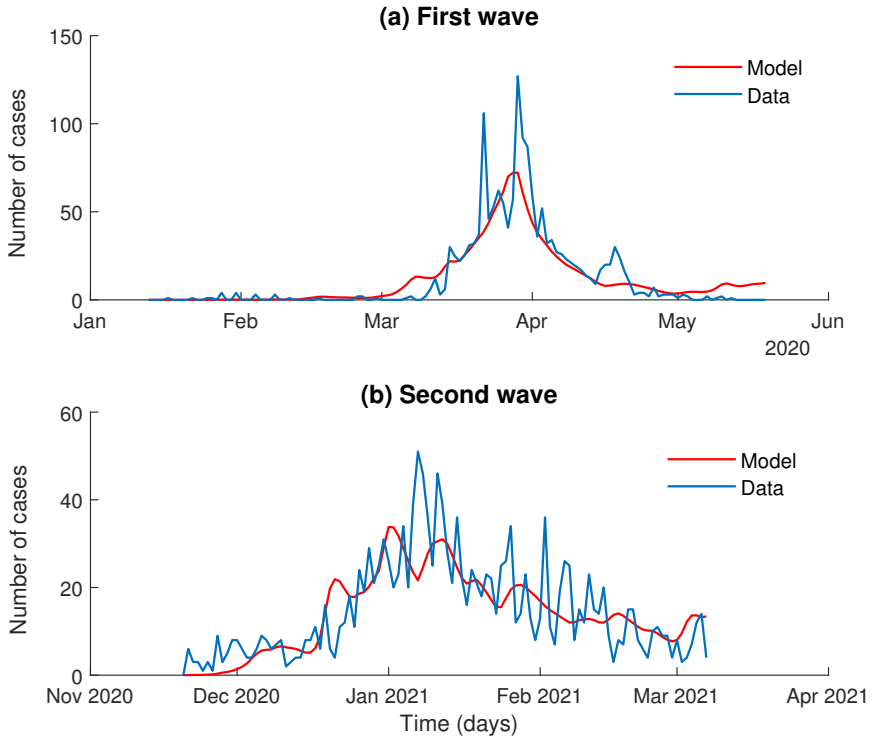

Figure 3. Model fitting of the first and second waves of the COVID-19 pandemic in Bangkok.

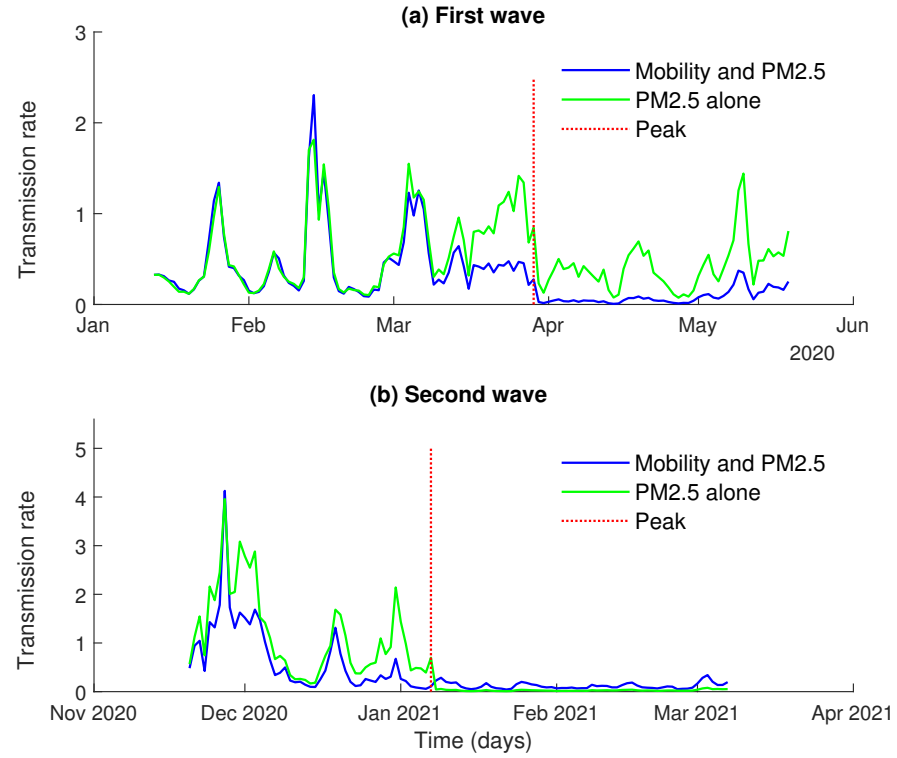

Figure 4. Estimated transmission rate for (**a**) the first wave, and (**b**) the second wave. Green line shows the estimated transmission rate without the effect of mobility. Vertical line separates the ascending and descending phases.

In Figure 4b, the distinction between $\beta(t)$ and pure PM2.5 can be clearly detected in the ascending phase. As we mentioned, the mobility component was lower than in the first wave. After the peak, however, the scaling effect of the mobility component reversed, i.e., the value of the mobility component was greater than that of the first wave, and the percent change increased. This low level of transmission was mainly caused by the baseline value.

We now predict the basic reproduction numbers based on the present model. By using the estimated parameters, we obtain $R_0 = 2.37$, for the first wave, and $R_0 = 3.512$ for the second wave. It is seen that the estimated R_0 in the first wave is close to, but a bit lower than, the value obtained in previous studies [26,32,36]. The present model allows calculating the time-dependent reproduction number shown in Formula (5), in which the dynamic of R_t is identical to the change in $\beta(t)$, but scaled by 7.27.

4. Discussion

We used a mixture of data-based and compartmental-based modeling to disclose the relationship between the infection rate of COVID-19 and the series of external inputs that partly captured the behavioral response of people to the emerging and reemerging pandemics, including the influence of environmental conditions. The dynamic of the transmission rate was assumed to be proportional to the product of a linear mobility function and the power law of PM2.5, where the proportional constant determined the baseline value. The daily confirmed case data during the two outbreaks in Bangkok 2020–2021 was used as a case study. The influence of mobility and PM2.5 was separately analyzed for the periods of epidemic growth and decay. The time series of mobility data during the two outbreaks displayed similar patterns; i.e., a down and up trend in the percentage change in the mobility volume. This reflects the strength of the lockdown measures and the anxiety of people about the new threat.

The PM2.5 data show bi-week fluctuations, in which the average concentration in the second wave was relatively high. The results showed that the transmission rate was positively correlated with mobility, except for the last period, while the presence of PM2.5 increased the baseline value of transmission. However, the model predicted a negative association between PM2.5 and the transmission rate. For example, we found that the transmission rate dropped by 6.2% as the concentration of PM2.5 increased 1 $\mu g/m^3$ during the ascending phase of the first wave. Although several studies have pointed out that PM2.5 could be associated with the 15.08% increase in COVID-19 cases [3], the mechanical causation of mobility's role in the infection requires deeper investigation. Nevertheless, our findings conform to studies in Bangkok and New York, in which the Spearman's rank correlation coefficient indicated that COVID-19 cases were negatively correlated with PM2.5 [8,9].

We have shown that the transmission rate in the first wave positively correlated with mobility, even though it presented a downtrend from the beginning of the year. However, it is difficult to evaluate the contribution of mobility to the growth of the epidemic in the first wave, since the recovery period of mobility occurred after the outbreak had ended. The transmission rate dropped on average by 1.25% for the ascending phase, and 8.32% for the descending phase, as the mobility decreased by 1%. Compared to the second wave, the decrease rate of mobility in the first wave was relatively low. The impact of mobility in the early phase was very low, unless the percentage change was lower than 50%. The main factor that dominated the reduction in the ascending phase was the baseline transmission. To achieve the goal of $R_t < 1$, the model suggested that $\beta(t)$ had to be less than 0.13. While PM2.5 magnified the baseline value, the mobility was low enough to keep $R_t < 1$ in the last phase.

In the second wave, however, a positive association with mobility was only detected in the ascending phase. The transmission rate decreased on average by 3.28% as the mobility dropped by 1%. Compared with the first wave, the larger reduction was due to the short period of the downtrend in mobility, which reflects the weaker control measures. It can be seen that the minimum mobility was higher on average than the minimum in the first

wave. Nevertheless, it is remarkable that the estimated value of the basic reproduction number in the second wave was greater than in the first wave, even though the reduction in mobility had a greater impact. This was because of the baseline value and the scaling effect of PM2.5. The negative association of mobility in the last phase may have been the result of the concurrence of the decline period in daily confirmed cases and the period of increasing mobility, which came faster than in the first wave. The transmission rate dropped on average by 1.64% for the descending phase as mobility increased by 1%. Therefore, we can observe that the effect of mobility in this phase was reversed.

In summary, the results potentially support the general theory about the temporal effect of mobility on the transmission of COVID-19, especially the decreasing phase of mobility. However, the results also strongly depend on the time period and the characteristics of the case data. Thus, a further analysis of the data correlation might help to confirm the disclosed relationship. For the mobility function, we observed that if $b > 1$, then the reduction in the rate of infection by mobility was greater for $M(t) < 100\%$, compared with the case $0 < b < 1$. On the contrary, enhancing the rate of infection through mobility was greater for $M(t) > 100\%$, compared with the case $0 < b < 1$. While the role of PM2.5 in transmission is controversial, our results also support the recent findings about the negative effect of PM2.5. The technical reason behind this might concern the limitations of the models. The simple form of the functions, adopted for the sake of simplicity, and the structure of the epidemic model was kept to a minimum, just to be sufficient, to present the salient features of the transmission of COVID-19 at a large scale and appropriate to the temporal dynamic of the epidemic. This would allow a more complex extension, such as the effect of vaccination, the combination of non-pharmaceutical measures, social behavior, and other pollution factors such as PM10, carbon monoxide, surface ozone, sulfur dioxide, etc. Such possible extensions could easily be made through restructuring the model equations and modifying the time-dependent transmission rate. For the latter, possible additional parameters describing the intervention such as contact tracing, isolation, vaccination, travel restriction, face mask wearing, and social distancing could be included in the Formula (2).

It would also be possible to consider the sensitivity to parameters and uncertainty in the model output; i.e., how the estimated results changed with respect to the small change in known parameter values. If information about the distributions of the input parameters is known, the sensitivity measure could account for the simultaneous variation in input parameters. In this study, one could examine further the uncertainty of the results subject to small variations in the asymptomatic ratio, the infectious period, and the initial conditions of the dynamic model.

The results of this study also motivate a future question about how the contact rate, transmission probability, and the mobility interacted through environmental changes. However, the need for further data and information about the relevant variables and parameters may be a trade-off, with the possibility of bias and instability of estimation.

Author Contributions: Conceptualization, K.P. and N.P.; methodology, K.P.; software, R.C.; validation, K.P., R.C. and N.P.; formal analysis, K.P.; investigation, K.P., R.C. and N.P.; writing—original draft preparation, K.P.; writing—review and editing, K.P.; visualization, R.C. and K.P.; supervision, N.P.; funding acquisition, K.P. All authors have read and agreed to the published version of the manuscript.

Funding: This research was financially supported by the Thailand Science Research and Innovation (TSRI) National Science, Research and Innovation Fund (NSRF) (Fiscal Year 2022) grant number 2313271.

Institutional Review Board Statement: Not applicable.

Informed Consent Statement: Not applicable.

Data Availability Statement: Publicly available datasets were analyzed in this study. This data can be found at http://air4thai.pcd.go.th, and https://data.go.th/dataset/covid-19-daily.

Conflicts of Interest: The authors declare no conflict of interest.

Abbreviations

The following abbreviations are used in this manuscript:

COVID-19	Coronavirus disease 2019
PM2.5	Particulate matter with a diameter of 2.5 micrometers
AIC	Akaike information criterion
CI	Confidence interval

Appendix A

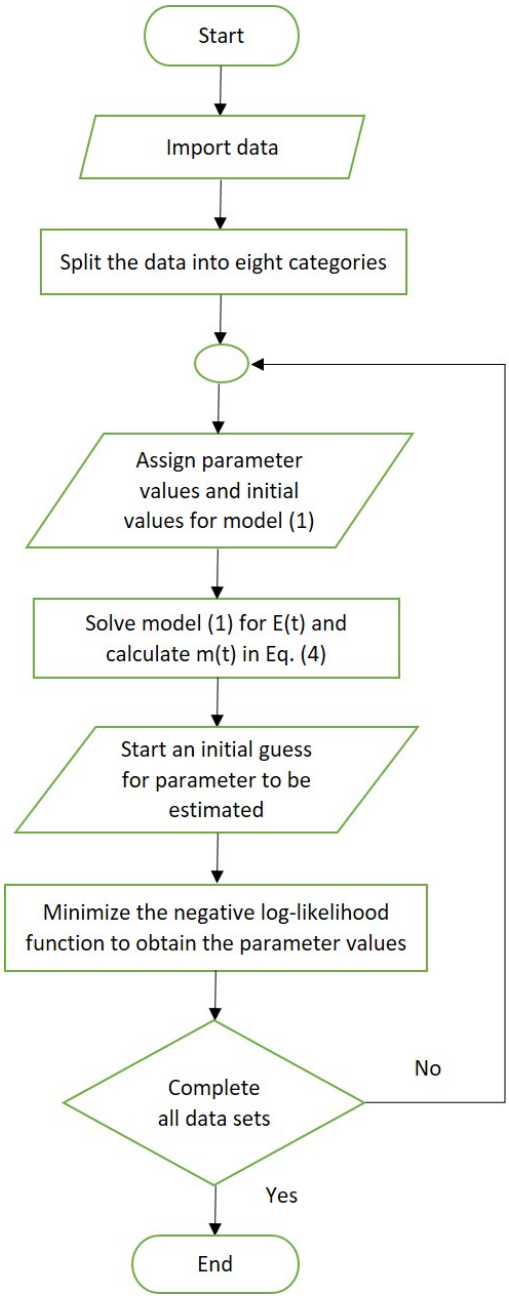

Figure A1. Flowchart of parameter estimation process.

Table A1. Summary of variables and parameters used in this study.

Symbol	Definition	Value	Reference
	Variable/function		
$S(t)$	number of susceptible individuals at time t		
$E(t)$	number of exposed individuals at time t		
$I_a(t)$	number of asymptomatic patients at time t		
$I_s(t)$	number of symptomatic patients at time t		
$M(t)$	percent change of human mobility at time t		
$P(t)$	averaged PM2.5 concentration at time t		
$\beta(t)$	transmission rate at time t		
$m(t)$	mean number of daily reported cases		
R_t	time-dependent reproduction number		
	Parameter		
N	Bangkok population	5,666,264	[37]
c	ratio of transmissibility between asymptomatic and symptomatic case	0.418	[33]
α	asymptomatic ratio	0.3	[34]
γ_a	recovery rate of asymptomatic infection	0.2 day^{-1}	[26]
γ_s	recovery rate of symptomatic infection	0.10526 day^{-1}	[26]
σ	outflow rate of exposed state	$1/5.2$ day^{-1}	[26]
θ	fraction of new infections that have been reported	0.2	[32]
β_0	transmission rate at 100% mobility change per one unit of PM2.5 concentration	estimate	
b	linear coefficient in mobility function	estimate	
d	exponent of scaled PM2.5 concentration	estimate	
R_0	basic reproduction number	estimate	

References

1. Urrutia-Pereira, M.; Mello-da Silva, C.; Solé, D. COVID-19 and air pollution: A dangerous association? *Allergol. Immunopathol.* **2020**, *48*, 496–499. [CrossRef] [PubMed]
2. Solimini, A.; Filipponi, F.; Fegatelli, D.; Caputo, B.; De Marco, C.M.; Spagnoli, A.; Vestri, A. A global association between COVID-19 cases and airborne particulate matter at regional level. *Sci. Rep.* **2021**, *11*, 6256. [CrossRef] [PubMed]
3. Meo, S.; Al-khlaiwi, T.; Ullah, C. Effect of ambient air pollutants PM2.5 and PM10 on COVID-19 incidence and mortality: Observational study. *Eur. Rev. Med. Pharmacol. Sci.* **2021**, *25*, 7553–7564. [CrossRef] [PubMed]
4. Ali, N.; Islam, F. The Effects of Air Pollution on COVID-19 Infection and Mortality—A Review on Recent Evidence. *Front. Public Health* **2020**, *8*, 580057. [CrossRef] [PubMed]
5. Wang, B.; Liu, J.; Li, Y.; Fu, S.; Xu, X.; Li, L.; Zhou, J.; Liu, X.; He, X.; Yan, J.; et al. Airborne particulate matter, population mobility and COVID-19: A multi-city study in China. *BMC Public Health* **2020**, *20*, 1585. [CrossRef]
6. Czwojdzińska, M.; Terpińska, M.; Kuźniarski, A.; Płaczkowska, S.; Piwowar, A. Exposure to PM2.5 and PM10 and COVID-19 Infection Rates and Mortality: A one-year observational study in Poland. *Biomed. J.* **2021**, *44*, S25–S36. [CrossRef]
7. Setti, L.; Passarini, F.; Gennaro, G.D.; Barbieri, P.; Licen, S.; Perrone, M.G.; Piazzalunga, A.; Borelli, M.; Palmisani, J.; Gilio, A.D.; et al. Potential role of particulate matter in the spreading of COVID-19 in Northern Italy: First observational study based on initial epidemic diffusion. *BMJ Open* **2020**, *10*, e039338. [CrossRef]
8. Sangkham, S.; Islam, M.A.; Sarndhong, K.; Vongruang, P.; Hasan, M.N.; Tiwari, A.; Bhattacharya, P. Effects of fine particulate matter (PM2.5) and meteorological factors on the daily confirmed cases of COVID-19 in Bangkok during 2020–2021, Thailand. *Case Stud. Chem. Environ. Eng.* **2023**, *8*, 100410. [CrossRef]
9. Adhikari, A.; Yin, J. Short-Term Effects of Ambient Ozone, PM2.5, and Meteorological Factors on COVID-19 Confirmed Cases and Deaths in Queens, New York. *Int. J. Environ. Res. Public Health* **2020**, *17*, 4047. [CrossRef]
10. Howard, D.; Giani, P.; Castruccio, S.; Anav, A.; Hu, W.; Crippa, P. Short-term and long-term health impacts of air pollution reductions from COVID-19 lockdowns in China and Europe: A modelling study. *Lancet Planet. Health* **2020**, *4*, e474–e482. [CrossRef]
11. Wetchayont, P. Investigation on the Impacts of COVID-19 Lockdown and Influencing Factors on Air Quality in Greater Bangkok, Thailand. *Adv. Meteorol.* **2021**, *2021*, 6697707. [CrossRef]
12. Faridi, S.; Yousefian, F.; Janjani, H.; Niazi, S.; Azimi, F.; Naddafi, K.; Hassanvand, M.s. The effect of COVID-19 pandemic on human mobility and ambient air quality around the world: A systematic review. *Urban Clim.* **2021**, *38*, 100888. [CrossRef] [PubMed]

13. Hu, T.; Wang, S.; She, B.; Zhang, M.; Huang, X.; Cui, Y.; Khuri, J.; Hu, Y.; Fu, X.; Wang, X.; et al. Human mobility data in the COVID-19 pandemic: Characteristics, applications, and challenges. *Int. J. Digit. Earth* **2021**, *14*, 1126–1147. [CrossRef]
14. Strzelecki, A. The Apple Mobility Trends Data in Human Mobility Patterns during Restrictions and Prediction of COVID-19: A Systematic Review and Meta-Analysis. *Healthcare* **2022**, *10*, 2425. [CrossRef] [PubMed]
15. Miller, A.C.; Foti, N.J.; Lewnard, J.A.; Jewell, N.P.; Guestrin, C.; Fox, E.B. Mobility trends provide a leading indicator of changes in SARS-CoV-2 transmission. *medRxiv* **2020**. [CrossRef]
16. Noland, R.B. Mobility and the effective reproduction rate of COVID-19. *J. Transp. Health* **2021**, *20*, 101016. [CrossRef]
17. Oztig, L.; Askin, O. Human Mobility and COVID-19: A Negative Binomial Regression Analysis. *Public Health* **2020**, *185*, 364–367. [CrossRef]
18. Mileu, N.; Costa, N.; Marques da Costa, E.; Alves, A. Mobility and Dissemination of COVID-19 in Portugal: Correlations and Estimates from Google's Mobility Data. *Data* **2022**, *7*, 107. [CrossRef]
19. Bergman, N.K.; Fishman, R. Correlations of mobility and Covid-19 transmission in global data. *PLoS ONE* **2023**, *18*, e0279484. [CrossRef]
20. Imai, C.; Armstrong, B.; Chalabi, Z.; Mangtani, P.; Hashizume, M. Time series regression model for infectious disease and weather. *Environ. Res.* **2015**, *142*, 319–327. [CrossRef]
21. Zhang, M.; Wang, S.; Hu, T.; Fu, X.; Wang, X.; Hu, Y.; Halloran, B.; Li, Z.; Cui, Y.; Liu, H.; et al. Human mobility and COVID-19 transmission: A systematic review and future directions. *Ann. GIS* **2022**, *28*, 501–514. [CrossRef]
22. Tantrakarnapa, K.; Bhopdhornangkul, B. Challenging the spread of COVID-19 in Thailand. *One Health* **2020**, *11*, 100173. [CrossRef]
23. Srichannil, C. The COVID-19 pandemic and Thailand: A psychologist's viewpoint. *Psychol. Trauma Theory Res. Pract. Policy* **2020**, *12*, 485–487. [CrossRef] [PubMed]
24. Triukose, S.; Nitinawarat, S.; Satian, P.; Somboonsavatdee, A.; Chotikarn, P.; Thammasanya, T.; Wanlapakorn, N.; Sudhinaraset, N.; Boonyamalik, P.; Kakhong, B.; et al. Effects of public health interventions on the epidemiological spread during the first wave of the COVID-19 outbreak in Thailand. *PLoS ONE* **2021**, *16*, e0246274. [CrossRef] [PubMed]
25. Dechsupa, S.; Assawakosri, S.; Phakham, S.; Honsawek, S. Positive impact of lockdown on COVID-19 outbreak in Thailand. *Travel Med. Infect. Dis.* **2020**, *36*, 101802. [CrossRef]
26. Mahikul, W.; Chotsiri, P.; Ploddi, K.; Pan-ngum, W. Evaluating the Impact of Intervention Strategies on the First Wave and Predicting the Second Wave of COVID-19 in Thailand: A Mathematical Modeling Study. *Biology* **2021**, *10*, 80. [CrossRef]
27. Chirasophon, S.; Pochanart, P. The Long-term Characteristics of PM10 and PM2.5 in Bangkok, Thailand. *Asian J. Atmos. Environ.* **2020**, *14*, 73–83. [CrossRef]
28. Rezaee, Z.; Aliabadi, S.; Dorestani, A.; Rezaee, N.J. Application of Time Series Models in Business Research: Correlation, Association, Causation. *Sustainability* **2020**, *12*, 4833. [CrossRef]
29. Girardi, P.; Gaetan, C. An SEIR Model with Time-Varying Coefficients for Analyzing the SARS-CoV-2 Epidemic. *Risk Anal.* **2023**, *43*, 144–155. [CrossRef]
30. Lingcai, K.; Duan, M.; Shi, J.; Hong, J.; Chang, Z.; Zhang, Z. Compartmental structures used in modeling COVID-19: A scoping review. *Infect. Dis. Poverty* **2022**, *11*, 72. [CrossRef]
31. Flanders, W.D.; Kleinbaum, D.G. Basic Models for Disease Occurrence in Epidemiology. *Int. J. Epidemiol.* **1995**, *24*, 1–7. [CrossRef] [PubMed]
32. Patanarapeelert, K.; Songprasert, W.; Patanarapeelert, N. Modeling Dynamic Responses to COVID-19 Epidemics: A Case Study in Thailand. *Trop. Med. Infect. Dis.* **2022**, *7*, 303. [CrossRef] [PubMed]
33. Nakajo, K.; Nishiura, H. Transmissibility of asymptomatic COVID-19: Data from Japanese clusters. *Int. J. Infect. Dis.* **2021**, *105*, 236–238. [CrossRef] [PubMed]
34. Nishiura, H.; Kobayashi, T.; Miyama, T.; Suzuki, A.; Jung, S.; Hayashi, K.; Kinoshita, R.; Yang, Y.; Yuan, B.; Akhmetzhanov, A.R.; et al. Estimation of the asymptomatic ratio of novel coronavirus infections (COVID-19). *Int. J. Infect. Dis.* **2020**, *94*, 154–155. [CrossRef]
35. Ma, J. Estimating epidemic exponential growth rate and basic reproduction number. *Infect. Dis. Model.* **2020**, *5*, 129–141. [CrossRef]
36. Rotejanaprasert, C.; Lawpoolsri, S.; Pan-ngum, W.; Maude, R.J. Preliminary estimation of temporal and spatiotemporal dynamic measures of COVID-19 transmission in Thailand. *PLoS ONE* **2020**, *15*, e0239645. [CrossRef]
37. Demography Population and Housing Branch. Available online: http://statbbi.nso.go.th/staticreport/page/sector/en/01.aspx (accessed on 7 April 2022).